1/7/91

PROPOSAL 838

Double-Spin Asymmetry (A_{LL}) Measurements in Charmonium Production at 200 GeV/c

by

M. E. Beddo, D. P. Grosnick, D. A. Hill, D. Lopiano, H. Spinka,
D. G. Underwood, and A. Yokosawa
Argonne National Laboratory, Argonne, Illinois, USA

J. Bystricky, F. Lehar, and A. de Lesquen
CEN, Saclay, France

D. C. Carey, and D. Cossairt,
Fermi National Accelerator Laboratory, Batavia, Illinois, USA

N.I. Belikov, A. A. Derevschikov, D. A. Grachov, Yu. A. Matulenko,
A. P. Meschanin, S. B. Nurushev, D. I. Patalakha, V. L. Rykov, R. A. Rzaev,
V. L. Solovyanov, L. F. Soloviev, and A. N. Vasiliev
Institute of High Energy Physics, Serpukhov, USSR

N. Akchurin, and Y. Onel
Department of Physics, University of Iowa, Iowa City, Iowa, USA

H. Enyo, H. Funahashi, Y. Goto, K. Imai, Y. Itow, S. Makino,
A. Masaike, N. Saito, and S. Yamashita
Kyoto University, Kyoto, Japan

R. Takashima
Kyoto University of Education, Kyoto, Japan

F. Takeutchi
Kyoto-Sangyo University, Kyoto, Japan

K. Kuroda, and J. Soffer
LAPP-ANNECY, France

J. Jarmer, S. Penttila, and N. Tanaka
Los Alamos National Laboratory, Los Alamos, New Mexico, USA

G. Salvato, and A. Villari
INFN-Messina, Italy

G. Burleson, G. S. Kyle, S. Mukhopadhyay, and M. Rawool-Sullivan
Department of Physics, New Mexico State University, New Mexico, USA

T. Maki
University of Occupational and Environmental Health, Kita-Kyushu, Japan

N. Tamura
Okayama University, Okayama Japan

T. Yoshida
Osaka City University, Osaka Japan

Y. Mizuno
RCNP, Osaka University, Osaka, Japan

M. D. Corcoran, C. Nguyen, J. B. Roberts, and J. L. White
T. W. Bonner Nuclear Laboratory, Rice University, Houston, Texas, USA

M. Georgi, A. Martin, A. Penzo, P. Schiavon, and A. Zanetti
University of Trieste, and Instituto Nazionale di Fisica Nucleare,
Trieste, Italy

G. Pauletta
Instituto di Fisica, University di Udine, 33100 Udine, Italy

January 02, 1991

Cospokespersons:
A. Masaike (Japan)
S. Nurushev (USSR)
A. Yokosawa,
Argonne National Laboratory
(708) 972-6311

Abstract

We propose to simultaneously measure the asymmetry parameter A_{LL} for inclusive χ_2, J/ψ, and in addition π° production by utilizing the 200 GeV/c polarized-proton beam on a polarized target. Our aim is to obtain the gluon-spin information from these three processes in order to determine what portion of the proton spin is carried by gluons. We anticipate obtaining significant numbers of χ_2 and J/ψ events. The statistical errors on A_{LL} will be small enough for the determination of the spin-dependent gluon structure function in a specific x range where the gluon polarization is expected to be sizeable. We anticipate the χ_2 channel to be particularly useful for this purpose. This would be the world's first measurement of gluon-spin information and of spin effects in charmed-particle production.

TABLE OF CONTENTS

Page

I. Introduction 4

II. Physics Goals 5

1) $\chi_2(3555)$ Production
2) J/ψ Production
3) π° Production

III. Theoretical Studies on A_{LL} in Charmonium Production 9

IV. Experimental Setup 11

1. Beam and Target
2. Detectors
3. χ_1 and χ_2 Separation
4. Scintillator Pad

V. Trigger Scheme and Trigger Rate 15

VI. Event Rate 17

VII. Background Rate 19

VIII. Determination of $\Delta G/G(x)$ 22

IX. Summary 23

References 25

Appendix I Uniqueness of 200-GeV/c Polarized Beam 27

Appendix II Determination of $R = f_-/f_+$ 28

Appendix III Expected Errors on A_{LL} in π° Production 29

Appendix IV CsI EM Calorimeter 30

Appendix V Reconstruction Efficiency 33

Appendix VI Comparison of E-673 Results (Ref. 4) and This Proposal 35

Appendix VII What is Needed 36

I) Introduction

Results from the recent experiment[1] to determine a spin-dependent structure function $(g_1^p(x))$ of the proton have been interpreted to mean that the proton spin may not be due to the helicity of its constituent quarks, as was generally believed earlier. Instead, most of the proton spin may be due to gluons (anomalous gluon polarization with several units of $\hbar$) and/or orbital angular momentum of the constituent partons.[2] This situation is referred to as the "proton-spin crisis".

In order to investigate this crisis, a number of quark-spin experiments are being prepared at LEP, SPS, HERA, and SLAC using polarized electron or muon beams. These experiments will measure only the quark-spin distribution in the polarized proton and neutron but will not measure the gluon-spin distributions.

A unique opportunity exists at Fermilab to utilize the present 200-GeV/c polarized proton beam to obtain gluon-spin information in inclusive production of χ_2, J/ψ, and π° simultaneously. Specifically we will measure the double-spin parameter A_{LL} with a longitudinally polarized proton beam on a longitudinally polarized nucleon target:

$$A_{LL}\ (p^\uparrow N^\uparrow \rightarrow \chi_2 + X),$$
$$A_{LL}\ (p^\uparrow N^\uparrow \rightarrow J/\psi + X), \text{ and}$$
$$A_{LL}\ (p^\uparrow N^\uparrow \rightarrow \pi^\circ + X).$$

We will obtain enough χ_2 and J/ψ events needed to determine the gluon-spin structure function, $\Delta G/G(x)$, in a specific x range. Our prospect for extracting the gluon spin information from our measurements is discussed in Section III together with theoretical models. The χ_2 channel offers the

cleanest theoretical interpretation. The physics interpretation will be tested using production rates, and the signs and the magnitudes of the A_{LL} parameters for χ_2, J/ψ, and possibly χ_1 production. Further consistency checks can be performed with charmonium decay angular distributions, and A_{LL} for π° production.

The proposed measurements can be done only at Fermilab and are complementary to the above mentioned quark-spin experiments. Higher-energy and higher-intensity polarized proton beams may be constructed, for instance, at the Tevatron, but not within the next several years. Prior to that, it is crucial to carry out measurements providing quantitative insight on the contribution to the proton spin from the gluons.

The Fermilab MP 200-GeV/c polarized beam offers an ideal kinematic domain in order to carry out the charmonium-production experiments as described above. A possible polarized collider, such as RHIC, will not be suited to study the gluon-spin distribution through charmonium production because of kinematical reasons, as shown in Appendix I.

II) Physics Goals

1) χ_2 (3555) Production

We propose to measure the A_{LL} asymmetry in χ_2 production via the $\chi_2 \rightarrow J/\psi + \gamma \rightarrow e^+e^-\gamma$ channel. The measured experimental asymmetry is given by

$$A_{LL} = \left[1/(P_B \cdot P_T^{eff})\right] \frac{I\,(++) - I\,(+-)}{I\,(++) + I\,(+-)} , \qquad (1)$$

where P_B is the beam polarization, P_T^{eff} is the effective target polarization and I (++), I (+-) are the number of events normalized to the incident beam. The helicity states (++) and (+-) correspond to $[\vec{\leftarrow}]$ and $[\vec{\rightarrow}]$ respectively,

where arrows indicate the beam and target spin direction in the laboratory system.

The hadronic production of the χ states involves three parton fusion diagrams: gluon fusion, light quark annihilation, and color evaporation.[3,4]

PROCESS	DIAGRAM	PROCESS	DIAGRAM
GLUON FUSION	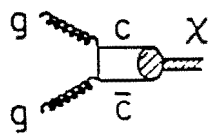	COLOR EVAPORATION	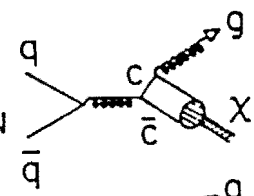
LIGHT QUARK FUSION	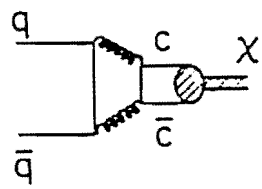		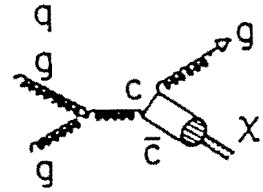

It is generally believed that the χ_2 (3555) state is mainly produced by gluon-gluon fusion. In Eq.(1), if the initial helicity state is (+-), then $J_z = 2$ and this state produces χ_2. There is an experimental result[4], although with limited number of events, suggesting that simple gluon fusion is sufficient to account for the χ_2 production in proton interactions at 200 GeV/c.

For clarity, we here discuss the experiment in terms of the gluon fusion model. Other possibilities are discussed later in this proposal.

Based on the gluon fusion model, the observable A_{LL} is related to the distribution function of a polarized gluon in a polarized proton (or nucleon) expressed as $G_+(x)$ and $G_-(x)$ with same- and opposite-sign helicities respectively.[5] The dependence is given by:

$$A_{LL}(x_F) = \hat{A}_{LL}\left[\frac{\Delta G}{G}(x_1) \cdot \frac{\Delta G}{G}(x_2)\right], \qquad (2)$$

where x_1, x_2, are the longitudinal-momentum fraction of gluons, x_F is the longitudinal fraction of the χ_2 and $x_F = x_1 - x_2$, $M^2_{\chi_2} = x_1 \cdot x_2 \cdot s$, $\Delta G/G(x) \equiv (G_+(x) - G_-(x))/(G_+(x) + G_-(x))$, $\hat{A}_{LL}$ is A_{LL} (χ_2) for two fully polarized gluons. $\hat{A}_{LL}$ is given by $(1 - R)/(1 + R)$, where R is the ratio of the squared matrix elements f_- (f_+) for the production of χ_2 out of two gluons with opposite- (same-) sign helicities, i.e. $J_z = 2$ $(J_z = 0)$.[5] $\hat{A}_{LL}$ is predicted to be -1 according to the gluon-fusion model in Ref. 6. We can test this prediction experimentally because the ratio $R = f_-/f_+$ can be determined from the unpolarized angular distribution of the χ_2 decay (by adding both spins) as[5]

$$\frac{1}{\sigma}\frac{d\sigma}{d\cos\theta} = \frac{1 - (1-R)\ 3/8\ (1 + \cos^2\theta)}{1 + R}, \qquad (3)$$

where θ is the angle between the photon and the beam momentum in the χ_2 rest frame. The determination of R is discussed in Appendix II.

In this experiment the separation of χ_1 (3510 MeV) and χ_2 (3555 MeV) is possible as described later. The matrix element for χ_1 production via gluon fusion is calculated to be zero according to the lowest-order QCD.[3] If few χ_1 events are detected, then gluon fusion is dominant in χ_2 production. If χ_1 events are significant, we may need to also include other processes in the calculations to determine $\Delta G/G$. Note that A_{LL} $(p^\uparrow N^\uparrow \to \chi_1 + X)$ and the $\chi_1 \to J/\psi + \gamma$ decay angular distribution will be measured simultaneously in this case, providing additional input for understanding the production process and the value of $\Delta G/G$. Possible interpretation of the experimental results is discussed in Section III.

2) <u>J/ψ Production</u>

We propose to measure the A_{LL} asymmetry in the J/ψ production via J/ψ →

e^+e^- channel. The A_{LL} is defined in Eq.(1) and will be measured simultaneously with the $\chi_2(3555)$ measurement. This measurement is complementary to the χ_2 experiment as discussed in the Section III. Predictions are made in terms of the gluon-spin distribution and a proposed production mechanism.

The advantage of this channel is that measurement is technically easier than that of χ_2 and several times more events can be accumulated than in the χ_2 channel. It also provides a further check of the charmonium-production mechanism (see Section III).

3) <u>π° Production</u>

The asymmetry A_{LL} in π° production has been described earlier in Refs. 7 and 8, where evaluation of QCD cross sections for definite helicity quarks and gluons is given. In the light of the EMC data[1] the most recent work was done by Ramsey and Sivers[9], who used the valence-quark spin-weighted distributions, $\Delta u_v(x,Q^2)$ and $\Delta d_v(x,Q^2)$ from Ref. 10. Their prediction using a QCD-based hard-scattering model gives large A_{LL} ($pp \rightarrow \pi^\circ x$) values if the gluons in a proton are highly polarized.

We will be able to measure the A_{LL} value with good accuracy up to $p_\perp = 5$ GeV/c where the QCD coupling constant $\alpha_s = 0.22$. Our recent measurements in A_N demonstrate the x_T scaling as shown in Fig. 1, suggesting that we may have reached a hard-scattering region near $p_T = 4$ GeV/c.

We have actually begun A_{LL} measurements at 200 GeV/c in $p^\uparrow p^\uparrow \rightarrow \pi^\circ x$ (E-704) during the 1990 fixed-target period. The data shown in Fig. 2 were taken simultaneously with other measurements requiring a low-intensity beam and therefore the errors are large. The expected statistical errors for the proposed run are shown in Fig. 2 as well as Appendix III.

III. Theoretical Studies on A_{LL} in Charmonium Production

1) Review of Theoretical Work

The A_{LL} in charmonium production has been theoretically discussed by a number of authors.[5-7,11] The latest work was done by Doncheski et al,[6] and Contogouris et al.[11] Their predicted results depend upon the theoretical assumptions for:

- $\Delta G/G(x)$ (gluon polarization), and
- charmonium production mechanism, which determines the sub-process double spin asymmetry $\hat{A}_{LL}$.

Large $\Delta G/G(x)$ values were recently proposed by several authors to compensate for the small value of the quark polarization discovered unexpectedly by the EMC group.[1] These assumptions[12-14] are summarized in Fig. 3 and these are all for big ΔG (anomalous large gluon polarization). Our proposed experiments measures $\Delta G/G(x)$ near $x = 0.18$, where the $\Delta G/G(x)$ is predicted to be 0.6 to 0.9.

In Refs. 6 and 11, A_{LL} in the charmonium production was calculated using these new $\Delta G/G(x)$ predictions. We discuss the charmonium production mechanisms that were employed in these references.

In Ref. 6, a perturbative QCD approach using quarkonium wavefunctions derived from non-relativistic potential models is employed to calculate $\hat{A}_{LL}$ for χ_2 and J/ψ. They assumed that the gluon-gluon fusion is dominant in χ_2 production. Hence, the first order $\hat{A}_{LL}$ is -1 for χ_2, as expected for the effective vertex of χ_2 production:

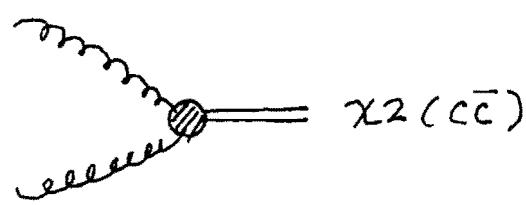

On the other hand, the $\hat{A}_{LL}$ for J/ψ is more complicated because direct J/ψ production is prohibited by C invariance. There are two major J/ψ production sources: (1) the χ_2 radiative decay, and (2) the color evaporation process $gg \to g + J/\psi$. The asymmetries of these two sources have to be combined to derive the $\hat{A}_{LL}$ of J/ψ. The $\hat{A}_{LL}$ for $gg \to g + J/\psi$ calculated in Ref. 6 is 0.0 to + 0.3, depending on the energies of incoming gluons, and will thus tend to dilute the above $\hat{A}_{LL}$ (χ_2) value. The A_{LL} predictions thus obtained are given in Fig. 4 and Fig. 5 for χ_2 and J/ψ, respectively. The $\Delta G/G(x)$ was quoted from Z. Kunszt.[13] For our proposed experiment with $\sqrt{s}$ = 19.4 GeV, we expect $A_{LL}(x_F = 0)$ = -24% for χ_2, and -18% for J/ψ.

In Ref. 11, the $\hat{A}_{LL}$ for charmonium production was calculated based on the QCD/semi-local duality approach together with the color re-arrangement by emission of soft gluons. In this model, once the $c\bar{c}$ pair is created in the $c\bar{c}$ mass range $(m_c + m_{\bar{c}}) \leq M \leq (m_D + m_{\bar{D}})$, then the emission and absorption of soft gluons can shift M so that the $c\bar{c}$ pair ends up in various charmonium states such as J/ψ, χ, and so on.

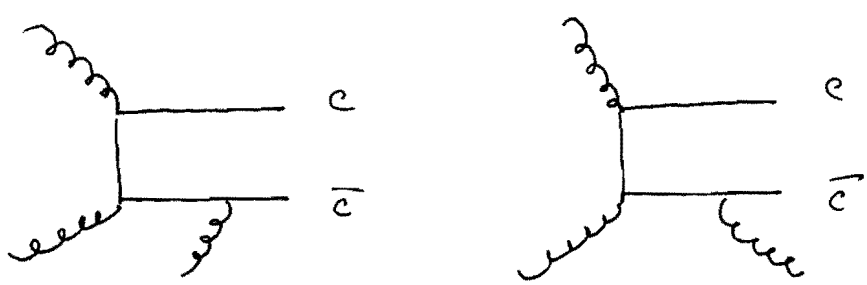

The charmonium A_{LL} predicted by this model is shown in Fig. 6 as a function of $\sqrt{s}$. The $\Delta G/G(x)$ was quoted from G. Altarelli (Solution (i) and Solution (ii).[12] For the proposed experiment with $\sqrt{s}$ = 19.4 GeV, this model predicts $A_{LL}(x_F = 0)$ = + 42% (solution (i)) or + 18% (solution ii)) for any charmonium

state. We note that the sign of A_{LL} in this model is opposite to that predicted in Ref. 6. This is because the sign of $\hat{A}_{LL}$ is opposite.

2) Interpretation of Experimental Results

Our proposed experiment has the capability to confirm the gluon fusion dominance by measuring the χ_1/χ_2 ratio. If the gluon fusion dominance is indicated by negligible χ_1 production, the determination of $\Delta G/G(x)$ is straight forward using the result of the A_{LL} measurement for χ_2 production; note that the proposed experiment even has a capability to confirm the predicted $\hat{A}_{LL}$ of χ_2 production by measuring the angular distribution of the photons from χ_2 radiative decays.

If other processes contribute, the measurements of χ_2, χ_1, and J/ψ become equally important. The A_{LL} (χ_2, χ_1, J/ψ) provide a test to various models, which predict opposite A_{LL} signs as discussed above. Thus, our proposed experiment will provide crucial information to understand the production mechanism, and will derive $\Delta G/G(x)$ eventually.

IV) Experimental Setup

1) Beam and Target

i) Polarized Beam

The polarized protons in the MP beam line are produced in the parity-nonconserving decays of Λ particles. In the unpolarized Λ rest frame, the decay $\Lambda \rightarrow p + \pi^-$ occurs isotopically and the decay-proton polarization is 64% with the spin direction along the proton momentum. A detailed description of the polarized beam is given in Ref. 15.

We request the following beam condition for an eight-month running period:

Primary Beam:	$4 \cdot 10^{12}$ incident protons/spill (the amount was based on the present Tevatron condition)
Beam Momentum:	200 GeV/c
Beam Intensity:	2.7×10^{7}/spill with 1 spill/60 sec, and beam polarization, $P_B = 0.45$

ii) Polarized Target

It was recently established[16] that substantial nuclear polarizations can be achieved in large targets of ^{6}LiD. To the extent that $^6Li^{\uparrow}$ can be viewed as He + $D^{\uparrow}$, as much as one-half of the nucleons are polarized in such a material. In most theoretical models, the gluon-spin distribution is the same for protons and neutrons. Thus interactions with either polarized nucleon are suitable for our measurements. Polarizations of $^6Li^{\uparrow}$ and $D^{\uparrow}$ approaching 70% should be achievable in the MP-9 polarized target, with the addition of a high-frequency (180 GHz) microwave source.

This special merit of the ^{6}LiD target arises from the much smaller "dilution factor", $1/\alpha$. This quantity $(1/\alpha)$ is related to A_{LL} and δA_{LL} as follows:

$$A_{LL} = \varepsilon(\text{raw asymmetry})/(P_B \cdot P_T^{eff}),$$

where P_T^{eff} (effective target polarization) = P_T/α and

$$\delta A_{LL} = \alpha \cdot \delta\varepsilon/(P_B \cdot P_T).$$

P_T is the nucleon polarization detected by nuclear magnetic resonance, $1/\alpha$ = 0.136 for the present E-704 polarized target, $C_5H_{12}O$, and $1/\alpha$ = 0.50 for the ^{6}LiD target. In terms of the running time required, there is a factor of

$(.50/.136)^2 \approx 14$ reduction. We also have less background from "unpolarized" target nuclei.

Characteristics of the polarized ^{6}LiD target (He + 2p↑ + 2n↑) are $\rho = 0.86/\text{gm/cm}^3$, 20-cm long, p_T (target polarization) = 70%, packing fraction of target beads = 64%.

2) Detectors

Our electromagnetic calorimeter consisting of 2,000 lead-glass counters is adequate for J/ψ and π° production measurements. For simultaneous measurements of the three processes proposed, we will provide an additional calorimeter with a good energy resolution for the γ detection.

A schematic view of the experimental arrangement is shown in Fig. 7, which consists of

- Electromagnetic calorimeters
- Proportional chambers
- Plastic scintillator-pad detector for the charmonium trigger

i) Electromagnetic Calorimeters

In order to separate χ_1 (3510 MeV) and χ_2 (3555 MeV) peaks, the energy resolution of the calorimeter is important, especially for the produced γ's. According to the decay kinematics of χ_2, the γ's are effectively detected at very forward angle (< 60 mrad). A calorimeter for detection of these γ's must have good energy resolution with fast response to handle the rates.

The central part (12 mrad < θ_{lab} < 60 mrad) of the calorimeter system consists of 400 blocks of pure CsI (3.8 x 3.8 x 40 cm^3 per each block) to ensure good energy resolution of the γ detection. There are two components (310 nm and 480-600 nm) of the CsI scintillation pulse. The fast component (310 nm) has a decay time of 20 nsec, while the slow component has a decay

time of a few μsec.[17] By filtering the slower component optically, pure CsI can be used as a high-resolution fast-response calorimeter. The energy resolution of 2% at E = 1 GeV has been measured.[17] The detailed description of the pure CsI calorimeter is given in Appendix IV including an estimate of the energy resolution.

The 2,000 lead-glass counters cover a large area (60 mrad < θ_{lab} < 130 mrad), and the combined lead-glass + CsI calorimeters cover x_F = -0.3 to 0.6. These lead glass blocks have been used in the earlier E-704 experiment for π° detection. The energy resolution is $(2 + 5/\sqrt{E})\%$.

At IHEP, Serpukhov, the GAMS-2000 experiment[18] used the same kind of lead-glass blocks with a similar setup as this proposal. The χ states have been detected by measuring e^+,e^-, and γ.[18] Clear J/ψ and χ peaks were observed with an open geometry configuration at a beam energy of 40 GeV.[18]

ii) Proportional Chambers

The proportional chambers placed between the target and the calorimeter serve to track e^+ and e^- particles and assure that there are no charged tracks in the γ direction. We use 4 sets of MWPC to measure electron trajectories. Each MWPC consists of XYUV planes with wire spacing of 1-2 mm. We require high efficiency in the MWPC's for high-rate measurements (few MHz). We provide an inactive area at the center of the MWPC's (< 10 mrad in lab.).

3) χ_1 and χ_2 Separation

The χ_2 mass resolution has been calculated by the Monte Carlo method with the following conditions. First of all, the J/ψ mass is reconstructed by measuring e^+e^- energies with the lead-glass or CsI calorimeter and measuring e^+e^- angles with 1-mm and 2-mm spacing MWPCs placed between the target and the calorimeter. The energy resolution of the lead-glass is $\sigma/E(GeV) = (2 + 5/\sqrt{E(GeV)})\%$ from the calibration data. The energy resolution of CsI is

assumed to be $\sigma/E(GeV) = (1 + 1/\sqrt{E(GeV)})\%$ (see Appendix IV). The J/ψ mass resolution is calculated to be 75 MeV (r.m.s.), which is dominated by the calorimeter energy resolution, rather than the MWPC spatial resolution.

After the J/ψ is reconstructed, the momenta of e^+ and e^- are constrained to give the exact J/ψ mass (3096 MeV) by scaling the energies of e^+ and e^-, while keeping the e^+e^- angles unchanged. The e^+e^- momenta thus constrained are combined with the momentum of the γ on the CsI to calculate the χ_2 mass. We assumed that the γ position in the CsI can be measured with 2 mm (r.m.s.) precision, which is the same precision as that confirmed for the lead-glass calorimeter used in the 1990 E-704 run. The χ_2 mass resolution obtained in this way is 10 MeV (r.m.s.), which is good enough to distinguish χ_2 (3555) from χ_1 (3510). The χ_1 and χ_2 mass spectrum shown in Fig. 8 was obtained in this Monte Carlo study. In comparison, if only lead-glass is used instead of CsI and lead glass, the χ_2 mass resolution is degraded to 20 MeV (r.m.s.), which makes χ_2 and χ_1 separation difficult.

4) Scintillator-Pad Detector

The scintillator-pad detector containing 100 pads has a segmented mosaic structure as shown in Fig. 7. It is placed 4.5 m from the target (2 m in front of the EM calorimeter). The size of the segmentation is determined to minimize chance coincidences of γ's with charged particles for the electron trigger described below.

V) Trigger Scheme and Trigger Rate

We trigger on J/ψ events with the p_T signals of e^+ and e^-. To obtain p_T signals from the calorimeter, we combine several lead-glass or CsI blocks into one super-block. Within each super-block, p_T signals are summed to provide a p_T (super-block) signal. In front of the calorimeter, we put the scintillator

pads to tag the charged particles. The size and position of each scintillator pad corresponds to each calorimeter super-block. The trigger requirements are:

- 2 or more electron candidates which have p_T(super-block) > 0.6 GeV and have hits on the corresponding separate scintillator pads,
- Σp_T (super-block) of the electron candidates being greater than 2.5 GeV.

These requirements are satisfied by 88% of the J/ψ's detected in the lead-glass and CsI calorimeter. The p_T correlation between e^+'s and e^-'s from J/ψ decays is shown in Fig. 9.

We discuss the trigger rate due to the background particles produced in 200-GeV proton-proton hard collisions, i.e. fake events. In this simulation the super block structure is simplified such that all the super blocks consist of $4 \times 4 = 16$ lead-glass or CsI blocks. We generated events using the LUND (PYTHIA) Monte Carlo program, and applied these trigger requirements to those events. The spectrum of hadron energy deposition in the lead-glass was quoted from S. Orito et al.[19] The same spectrum was assumed for CsI. All the secondary interactions (both electromagnetic and hadronic) of the outgoing particles in the target material were included in this calculation, using the GEANT3 program.

The trigger rate estimated in this way is 58 events/spill with 2.7×10^7 protons/spill incident on 20-cm long polarized target. About 35% of this trigger is by electrons from converted γ's, and the rest is by charged hadrons overlapped with γ's within the super-block. Our data read-out system can handle this trigger rate.

We describe the detail of the trigger scheme. To cope with the lateral shower spread, super blocks are overlapped with each other. Calorimeter

blocks at the boundary of the scintillator pad belong to two (or more) super blocks as shown in Fig. 10. If the electron hits the calorimeter block at the boundary, its p_T signal goes to two super blocks, and one of them is selected by the scintillator pad signal. The logic diagram is given in Fig. 11 showing the way to obtain Σp_T of the electron candidates.

A simple high-p_T trigger will be applied to detect π^o's and it will be similar to the one used in the 1990 run (E-704).

VI) Event Rate

The event rate of the J/ψ or χ_2 production is given by

$$\rho \cdot \ell \cdot N_A \cdot N_b \cdot B \cdot \sigma \cdot A \cdot \varepsilon \cdot \varepsilon',$$

where ρ is the target density, ℓ is the target length, N_A is Avogadro's number 6.02×10^{23}, N_b is the number of incident polarized protons, $B\sigma$ is the decay branching ratio times total cross section, A is the geometrical acceptance, ε is the trigger efficiency, and ε' is the product of operation and reconstruction efficiencies.

1) Beam (from page 11)

$N_b = (2.7 \cdot 10^7/\text{min}) \cdot (60\ \text{min/hr}) \cdot (24\ \text{hr/day}) \cdot (30\ \text{d/mo})$

$= 1.17 \cdot 10^{12}$ polarized protons/month

2) Target (from page 12)

$\rho \ell N_A = (0.86\ \text{gm/cm}^3) \cdot (20\text{cm}) \cdot (6.0 \cdot 10^{23}\ \text{nucleons/gm}) \cdot$

$(0.64 = \text{packing fract.}) = 6.6 \cdot 10^{24}\ \text{nucleons/cm}^2$

3) $B \cdot \sigma$

The branching ratio times J/ψ production cross section $B(J/\psi \rightarrow e^+e^-) \cdot \sigma(J/\psi)$ that we use in our event rate estimation is 10 nb which is the

average of Refs. 20 to 22. To estimate the $B\sigma$ for χ_2, i.e. $B(\chi_2 \to J/\psi + \gamma) \cdot B(J/\psi \to e^+e^-) \cdot \sigma(\chi_2)$, we referred to D. A. Bauer et al.[4]; $B \cdot \sigma(\chi 2) = 0.47 \cdot 10$ nb = 4.7 nb.

4) Acceptance and Trigger Efficiency

The geometrical acceptance was calculated by the Monte Carlo method, which resulted in 43% for J/ψ and 16% for χ_2. The trigger efficiency was 88% with the above trigger requirement (see Fig. 9). The product is $A\varepsilon = 0.16 \cdot 0.88$ (trig. eff.) = 0.14 for χ_2 production. The p_T and x_F were generated with $Ed^3\sigma/dp^3 \propto \exp(-2.05\ p_T)\ (1 - x_F)^{3.44}$ for both J/ψ and χ_2. The polar angle of the γ from the χ_2 decay was generated with $1 + \cos^2\theta_\gamma$ in the Gottfried-Jackson frame. An isotropic decay was assumed for $J/\psi \to e^+e^-$. The e^+ or e^- which hit either CsI or lead-glass were accepted. On the other hand, only γ's which hit CsI were accepted to get enough resolution to distinguish χ_2 from χ_1. The electromagnetic interactions of the outgoing e^+,e^-, and γ with the polarized target material are included in this Monte Carlo calculation, using the GEANT3 software package. So, the acceptances thus calculated include the loss of the particles due to the target material. The edge effect due to the beam hole of the calorimeter is also estimated by excluding one internal layer of CsI counters in the simulation, then $A\varepsilon$ will be 0.134 instead of 0.141.

From 1) to 4)

Using all the values given above, we obtain the following event rate: χ_2 rate = $(6.6 \cdot 10^{24}/cm^2)\ (1.17 \cdot 10^{12}/mo)\ (10 \cdot 10^{-33})\ (0.47)\ (0.14) = 5120$ events/month.

5) Operating Efficiencies

(ε_{beam} (acc. beam available) ≈ 0.8) $\cdot$ (ε_{exp} (MP beam, PPT operation, etc.) ≈ 0.8) = 0.64.

6) Reconstruction Efficiency

The reconstruction efficiency (tracking, γ detection, etc.) was estimated to be 50% as described in Appendix V.

7) Final Rate

Our final χ_2 rate will be 1640 events/month, and the $J/\psi \rightarrow e^+e^-$ rate will be 9,200 events/month.

8) Running Time

We assume an eight-month running period. We expect 13,000 $\chi 2$ events and 73,000 J/ψ events for this running period.

9) Expected Errors in A_{LL}

See Section VIII.

For comparison, we have found in the E-705 Proposal (a second generation experiment dedicated to charmonium hadronproduction) that they expected to have 38,000 J/ψ and 3,300 χ_2 for 750-hours running time using a 300-GeV proton beam (the interaction rates for E-705 and P-838 Proposals are scaled). Taking into account that our geometrical efficiency for J/ψ and χ_2 is twice the size as in the E-705 experiment, we can say that our event-rate estimate is several times more conservative than that for E-705. In Appendix VI we show that our estimate is consistent with the published result from the E-673 experiment.

In Appendix III we present our π° event-rate estimate which is based on our experience from the 1990 run.

VII) Background Rate

When we identify $J/\psi \rightarrow e^+e^-$ by reconstructing the e^+e^- invariant mass with the EM calorimeter, the mass spectrum is contaminated by charged hadron pairs, whose production cross section at 200 GeV at the J/ψ invariant mass region is a factor 6000 larger than that of the J/ψ. However, we can still

reject most of the hadron pairs, since the hadrons deposit only small fractions of their energies in the EM calorimeter and the hadron pair mass spectrum is concentrated into the lower mass region. Furthermore, we can reject more hadrons by applying a lateral shower spread cut, since the typical lateral spread of a hadronic shower is larger than that of an EM shower. According to V. A. Davydov et.al.[23], the hadron rejection factor by the lateral shower spread cut is 10 for each hadron. Then, for a hadron pair, a rejection factor of 10 x 10 = 100 is achieved.

To estimate this type of background rate, the proton-proton hard collision events were generated by LUND(PYTHIA) Monte Carlo. The method is similar to that we took in the trigger rate study discussed above. The hadron energy deposition in the calorimeter was generated according to S. Orito et.al.[19]. All the secondary interactions (both electromagnetic and hadronic) of the outgoing particles in the target material were included in this calculation using GEANT3. The lateral shower spread in the calorimeter was not generated in this calculation, but the following methods were temporarily taken to include the shower overlapping effects:

- The γ's were combined into one energy cluster if the distance between the γ's was less than 40 mm in the calorimeter. The distance of 40 mm was chosen because the two-γ separation efficiency is less than 50% if the distance is less than 40 mm.
- The charged particles were also combined into one energy cluster if they hit the calorimeter within 10 mm of each other. The value of 10 mm was chosen to allow for effects of δ-rays in the MWPC's.
- If a γ hit the calorimeter within 6 mm of a charged particle, the γ energy was added to the energy deposited by the charged particle. Since the calorimeter can determine the EM shower center with 2 mm

precision (r.m.s.), 6 mm is 3 σ's of the position resolution of the calorimeter.

Because of CPU time limitations, we have generated enough LUND(PYTHIA) events to correspond to 10.5 accepted J/ψ events. For all the charged particle pairs in these events, we applied the following p_T cuts:

- $p_{T1} > 0.6$ Gev and $p_{T2} > 0.6$ Gev,
- $p_{T1} + p_{T2} > 2.5$ Gev,

where p_{T1} and p_{T2} are the transverse momenta of the charged particles in the pair, which are determined by the energies in the calorimeter and the measured angles from the MWPCs. As mentioned in the previous section on the event rate, these cuts retain 88% of the real J/ψ's.

As a result, 29 fake J/ψ's were found in the invariant mass region 2.8-3.3 GeV. Of these 29 events, 21 were hadron pairs, and 8 hadron-electron pairs. The electrons are conversion electrons due to the interactions between the γ's from π°'s and the target material. Applying the lateral shower spread cut to each hadron (a reduction factor of 10), the number of fake J/ψ's is estimated to be $(21 \cdot 0.1 \cdot 0.1)/10.5 + (8 \cdot 0.1)/10.5 = 0.1$ per real J/ψ. No fake χ_2 events were found in these events.

When the χ_2 is reconstructed by combining a J/ψ with a γ, we can not distinguish the γ which originates in the χ_2 from the γ's which originate in other particles such as π°. The major χ_2 background source comes from the combination of a J/ψ and a wrong γ. This type of background rate was estimated by overlapping Monte Carlo generated J/ψ and χ_2 events with LUND(PYTHIA) minimum bias events. Following the results of Ref. 4, the χ_2 decay events ($\chi_2 \rightarrow J/\psi + \gamma$) and the direct J/ψ events are generated in the Monte Carlo program with an equal rate and these events are overlapped at

random with LUND(PYTHIA) minimum bias events. The mass spectrum of $J/\psi + \gamma$ obtained by analyzing these Monte Carlo events is shown in Fig. 12. In this analysis, we did not use the γ's which form π°'s on the calorimeter within its mass resolution. This type of background rate is estimated to be about 10% of the real χ_2 events.

VIII) Determination of $\Delta G/G$ (x)

In the gluon fusion process, the following relations hold:

$$x_F = x_1 - x_2,$$
$$M^2 = x_1 \cdot x_2 \cdot s, \tag{4}$$

where M is the χ_2 mass and s is the center of mass energy squared. These relations connect the measured x_F distribution of χ_2 with the gluon structure function via Eq. (2). Our geometrical acceptance centers near $x_F = 0$ where $x_1 = x_2 = 0.18$ as shown in Fig. 13.

What we measure is the integral of $[\Delta G/G\ (x_1)] \cdot [\Delta G/G\ (x_2)]$ over x_1 and x_2 with $M^2_{\chi_2} = x_1 \cdot x_2 \cdot s$. The combination of cross section and acceptance will cover roughly $0.03 < x_1 < 0.18$ and $0.18 < x_2 < 0.33$.

After integrating the x_F acceptance, 8 months of beam time will give a statistical error of δA_{LL} (given below) to $\pm$ 0.02 for J/ψ production and δA_{LL} to $\pm$ 0.06 for χ_2 production.

$\delta A_{LL} = \dfrac{1}{P_B \cdot P_T^{eff}} \cdot \dfrac{1}{\sqrt{I_{tot}}}$, where P_B is the beam polarization, P_T^{eff} is the effective target polarization, and I_{tot} is the total number of events.

As an example, if we assume $\Delta G/G(x) = 0.9$ at $x = 0.18$ and $\hat{A}_{LL} = -0.71$ ($R = 6.0$) in Eq.(2), we then obtain $A_{LL} = -0.58$. In this case, our measurement will yield $A_{LL} = -0.58 \pm 0.06$ or $(\Delta G/G)^2 = 0.81 \pm 0.08$.

IX) Summary

We propose to measure the double-spin asymmetry A_{LL} in charmonium and π° production. We anticipate 1,640 reconstructed χ_2 events/month and 9,200 J/ψ events/month. Using 8-months of beam time, the estimated δA_{LL} will be $\pm$ 0.06 for χ_2 production and $\pm$ 0.02 for J/ψ production.

If we observe that χ_1 production is negligible, we can determine the gluon-spin structure function, $(\Delta G/G)$, via the gluon fusion model. From the results of the proposed experiment, we will obtain the amplitude of $\Delta G/G$ which has not been measured before. The experimental results will either confirm or deny the "anomalous gluon polarization" suggested by the EMC results.

The signs and magnitudes of $A_{LL}(\chi_2)$ and $A_{LL}(J/\psi)$ will provide crucial information on the production mechanism(s), if χ_1 production is not negligible. We believe that the theoretical ambiguity existing for the charmonium production mechanism can be solved experimentally by our many independent measurements for the J/ψ and χ states. A large value of A_{LL} will indicate a sizeable $\Delta G/G$ independent of models.

Our simultaneous measurement of A_{LL} for π° production provides another measurement of the gluon polarization which is independent of the charmonium-production mechanisms.

The present understanding of the proton is incomplete as shown by the EMC measurements. It is important to resolve the fundamental uncertainties in the structure of the nucleon. If polarized protons are important for finding and studying new physics, the gluon-spin structure function will be

essential. The proposed measurements in charmonium production can only be done at Fermilab, and will not be feasible at a future high-energy polarized collider. Other gluon-spin experiments may be very far in the future.

References

1) J. Ashman et al., Phys. Lett. B206, 364 (1988); Nucl. Phys. B238, 1 (1989).

2) For instance, see S. J. Brodsky, J. Ellis, and M. Karliner, Phys. Lett. B206, 309 (1988).

3) S. D. Ellis et al., Phys. Rev. Lett. 36, 1263 (1976); C. E. Carlson and R. Suaya, Phys. Rev. D14, 3115 (1976); C. E. Carlson and R. Suaya, Phys. Rev. D18, 760 (1978); R. Baier and R. Ruckl, Z. Phys. C19, 251 (1983); V. Barger and A. D. Martin, Phys. Rev. D31, 1051 (1985).

4) D. A. Bauer et al., Phys. Rev. Lett. 54, 753 (1985).

5) J. L. Cortes and B. Pire, Phys. Rev. D38, 3586 (RC) (1988).

6) M. A. Doncheski and R. W. Robinett, Phys. Lett. B248, 188 (1990).

7) N. S. Craigie, K. Hidaka, M. Jacob, and R. M. Renard, Phys. Rep. 99C, 69 (1983).

8) J. Babcock et al., Phys. Rev. D19, 1483 (1979).

9) G. Ramsey and D. Sivers, Phys. Rev. to appear.

10) J. W. Qiu et al., Phys. Rev. D41, 65(1990).

11) A. P. Contogouris et al., Phys. Lett. B246, 523 (1990).

12) G. Altarelli and W. Stirling, Particle World 1, 40 (1989).

13) Z. Kunszt, Phys. Lett. B218, 243 (1989).

14) W. L. Berger and J. Qiu, Phys. Rev. D40, 778 (1989).

15) D. P. Grosnick et al., Nucl. Instr. and Meth. A290, 269 (1990).

16) P. Chaumette et al., Proc. Symp. on High Energy Spin Physics, Minneapolis, MN, September, 1988.

17) H. Kobayashi et al., Nucl. Instrum. and Meth., to appear.

18) F. Binon et al., Nucl. Phys. B239, 371 (1984).

19) S. Orito et al., Nucl. Instr. and Meth. 215, 93 (1983).

20) J. G. Bramson et al., Phys. Rev. Lett. 38, 1331 (1977).

21) K. J. Anderson et al., Phys. Rev. Lett. 42, 944 (1979).

22) J. Badier et al., Z. Phys. C20, 100 (1983).

23) V. A. Davydov et al., Nucl. Instr. and Meth. 145, 267 (1977).

24) B. Cox et al., N.I.M. 219, 487 (1984).

APPENDIX I

Uniqueness of 200 GeV/c Polarized Beam

We illustrate that the Fermilab 200-GeV/c polarized beam is in the unique energy region to investigate the gluon-spin distribution in the charmonium production through the gluon-gluon fusion process. In a lower energy region, the cross section becomes too small, and in a higher energy region like a polarized collider with $\sqrt{s} =$ 200 to 500 GeV, there will be the following kinematic restriction:

From *Eq.* (4) in section VIII, $M^2/s = x_1 \cdot x_2 \approx 0$ at collider energies. For a given x_F coverage, x_1 or x_2 is zero. So far, all the theoretical models predict $\Delta G/G = 0$ at $x = 0$. Therefore, no information is obtained on $\Delta G/G(x)$ because A_{LL} is proportional to $\Delta G/G(x_1) \cdot \Delta G/G(x_2)$.

APPENDIX II

Determination of $R = f_-/f_+$

The ratio $R = f_-/f_+$ in the gluon fusion model is determined by fitting the photon angular distribution with *Eq.* (3). The statistical error on R was estimated with Monte Carlo generated events.

First, χ_2 events were generated assuming $\chi_2(J_z = 2)/\chi_2(J_z = 0) = 6$, *i.e.* $R = 6$. The γ angular distributions for $\chi_2(J_z = 2)$ and $\chi_2(J_z = 0)$ are :

$$W_\gamma^2(\theta_\gamma) = \frac{3}{16\pi}(1 + cos^2\theta_\gamma),$$

$$W_\gamma^0(\theta_\gamma) = \frac{1}{2\pi} - \frac{3}{16\pi}(1 + cos^2\theta_\gamma),$$

respectively, according to J. L. Cortes and B. Pire.[5] The number of generated events was 12,000.

The raw angular distribution of the events accepted by the calorimeter was corrected by the angular acceptance. The corrected angular distribution was fitted

with $Eq.$ (3). As a result, the R was 5.78±0.69, consistent with the expected input value, 6. The $cos\ \theta_\gamma$ acceptance is given in Fig. 14, and the acceptance-corrected $cos\ \theta_\gamma$ distribution is shown in Fig. 15.

Assuming measured value of $A_{LL} = -0.58 \pm 0.06$ and $R = 5.78 \pm 0.69$, we obtain $(\Delta G/G) \cdot (\Delta G/G) = 0.81 \pm 0.09$, using all the x_F acceptance. The accepted x_F distribution is given in Fig. 13. The error of the gluon spin structure measurement is dominated by the error of A_{LL}, and insensitive to the error of R.

APPENDIX III

Estimate of expected errors in A_{LL} for π^0 production

The estimate is made under the following assumptions:

- the intensity of the polarized beam is 2.7×10^7 protons/spill;
- the beam polarization is 45 %;
- the target polarization is 70 %;
- the dilution factor is 2;
- the beam time is 8 months;
- the operation efficiency (the accelerator and the experiment) is 64 %.

p_T coverage GeV/c	number of π^0's	statistical error in A_{LL}, %
3 – 4	700,000	0.7
4 – 5	30,000	3.2
5 – 6	1,300	15.0

This estimate is based on our experience from the 1990 run.

APPENDIX IV

CsI EM calorimeter

For our physics goal the γ shower detector must have 1% resolution for 10 to 30 GeV photons. This requires the use of a scintillating material, rather than a Čerenkov shower detector. The comparison of scintillating materials is shown in the following table:

Material	SF6	CsI(pure)	BaF2	BGO
Rad. Length(cm)	1.70	1.86	2.1	1.1
Int. Length(cm)	13.8	22.6	18.8	13.7
Moliere rad(cm)	3.6	3.8	4.4	2.7
Density(g/cm^3)	5.20	4.51	4.87	7.13
Diffractive index	1.80	2.19	1.56	2.15
Rad/Int. length	0.095	0.082	0.11	0.08
# photon/MeV	-	2000	6500	8200
$d\sigma/E$(1GeV)	3.6%	2%		
decay const(nsec)	Čerenkov	10/36/1000	0.6/620	300
wave length(nm)	-	310/310/480-600	225/310	480

Comparison of fast scintillating materials along with SF6 lead glass.

We have chosen pure-CsI considering the following reasons.

- SPEED: Pure CsI has two components (310 nm and 480 – 600 nm) of scintillation light. The fast component (310 nm) has a decay time of 10 – 40 nsec, while the slow component has a decay time of $1-3$ μsec. By optically filtering out the slower component, pure CsI becomes a fast-response EM calorimeter, comparable to a Čerenkov shower counter.

- RESOLUTION: The CsI energy resolution of $\delta E/E = 2\%/E^{0.4}$ has been reported[17] in the energy range less than 1.2 GeV, which will provide sufficient resolution for our purpose. This measurement uses only the fast component, which is 80-85% of the total light emission. The other scintillators, BaF2 and BGO, can be superior in terms of energy resolution over the higher light emission. However, BaF2 can not be manufactured into a crystal long enough for our energy region, and BGO is too expensive and rather slow.

- HADRONIC RESPONSE: CsI has a larger ratio of the nuclear collision length to the radiation length, which should reduce hadronic background.

- MOLIERE RADIUS: Although BGO has very small Moliere radius, which determines the lateral size of the shower, CsI has comparable radius than the SF6, and is thus acceptable. Note that the Moliere radius of the E704 lead glass (SF5 equivalent) is 4.2 cm, while that of CsI is 3.8 cm. Thus we expect difficulties caused by two different types of material to be small and correctable.

Recently pure CsI has been studied extensively for the CP violation experiment at KEK[17]. They have used 7x7x30 cm^3 (16 radiation length) blocks and obtained the energy resolution mentioned previously. Although this length is not large enough for high energy γ (10-30) GeV, we have tested the same size CsI blocks with a 27 GeV electron beam in FNAL-MP9. We have obtained an energy resolution of 1.5%, as expected from longitudinal shower leakage. For a further test we have ordered 20 pieces of 3.8x3.8x40 cm^3 blocks corresponding to 21.5 radiation length.

A good linearity is also measured in the energy range less than 1.2 GeV. This is one of important test items for the higher energy region.

Radiation hardness of the CsI crystal is not clearly known. According to measurements at KEK, pure-CsI seems to be 10 times better than lead glass for radiation damage.

There are several known weaknesses of CsI. One is the rather large temperature

dependence for the amount of light emission (-1.5%/deg). The other weakness is an existing hygroscopic character, but much smaller than NaI. We are planning to make a hermetically-sealed, temperature-controlled box for the entire calorimeter.

For estimating the CsI energy resolution we have assumed that the constant term is 1% for our Monte Carlo studies. Fig.16 shows expected resolutions extrapolated by various assumptions from the low energy measurements. The E705 collaboration has tested their scintillation glass shower counter(18.5 radiation length), and obtained $1.64\% + 1.13\%/\sqrt{E}$ [24]. Their results are also plotted in the same figure.

The resolution of lead glass, SF6(21.8 radiation length) has been tested by Orito et al.[19]. They have observed $3.6\%/\sqrt{E}$ up to 60 GeV, implying the constant term to be less than 0.5% for their case. We note that the E705 counter has a shorter length than Orito et al., and our length is approximately the same as that of Orito et al. Thus our 1% assumption for the constant term should be a moderate one. Also note that E705 has succeeded to separate the χ_1 and χ_2 with their scintillation glass (private communication).

APPENDIX V

Estimation of χ_2 reconstruction efficiency

An estimate of the χ_2 reconstruction efficiency must include:

- the shower finding efficiency of the e^+e^- pair in the EM calorimeter,
- the shower finding efficiency of γ in the CsI EM calorimeter, and
- the tracking efficiency of the e^+e^- pair by the proportional chambers.

The efficiency for the EM showers ($e^+e^-\gamma$) has been estimated using a Monte Carlo method by superimposing the LUND(PYTHIA) minimum-bias events with the generated χ_2 events. The method dealing with the lateral shower spread was simplified such that the two showers are considered to be merged if the distance is within 5.7 cm (1.5 block size). The χ_2 events are considered to be lost if :

- the energy cluster of e^+, e^- or γ from a χ_2 is coalesced with another shower,
- the photon from the χ_2 forms a π^0 by chance when it is combined with another photons in the event.

The second criteria is included since we plan to remove the γ's that could possibly be from π^0 decays in the analysis. The χ_2 reconstruction efficiency estimated in this method is 71%. For reference, we show the average multiplicity on the calorimeter from the LUND minimum-bias events: The requirement should actually be different

	CsI	Lead glass
γ	2.4	1.7
e^+ or e^-	0.37	0.32
Charged Hadron	2.3	1.5
Neutral Hadron	0.17	0.10

for e^+e^- and for γ, because we do not need as high an energy resolution for electrons that could overlap with other particles. On the other hand, the energy resolution for the γ is crucial for the experiment and we are not able to allow any overlap of other particles. According to this criteria, the simulation has a rather severe constraint by requiring no overlap for all three showers.

We have also consulted the thesis by T.Lukens from E673 and checked their γ reconstruction efficiency. They determined the γ finding efficiency by "implanting" electron calibration data on to real dimuon- triggered events, and checked how well original photons are reconstructed with certain criteria. No overlap from other particles was allowed. Because of the geometrical difference a direct comparison to P838 is difficult. They have lead glass blocks with a cross section of 15×15 cm^2, which has an equivalent size of 5.7×5.7 cm^2 by projecting to 6.5m from the target compared to the proposed P838 setup. We have a finer segmentation (3.8×3.8 cm^2) than E673. Both of the calorimeters have a hole in the center. The hole is ± 4.4 *mrad* for E673 and ± 12 *mrad* for the present setup. We applied a larger central hole to "deaden" the calorimeter around the beam region. E673 has preconverters that gives another chance of overlapping showers. The P838 proposal improves the detector on these three point. However, due to the non magnetic configuration of P838, we must expect a higher flux of low-energy hadrons. If we take the results of their photon-finding efficiency, we expect a γ reconstruction efficiency of around 60%.

If we assume a 95% one-track efficiency for the chambers and by taking our MC results (71%), we obtain 63% ($0.95 \times 0.95 \times 0.71$) for the overall efficiency. If we again assume a 95% tracking efficiency for the chambers, a 95% efficiency for electron shower detection, and a 60% efficiency for the photon reconstruction from χ decay as suggested from E673, an overall efficiency of 48% ($0.95 \times 0.95 \times 0.95 \times 0.95 \times 0.6$) is found.

Finally, we have assumed 50% as the χ_2 reconstruction efficiency for our event rate estimation.

APPENDIX VI

Comparison of E673 Results (Ref. 4) and This Proposal

Yield $= L \cdot B\sigma \cdot A \cdot \epsilon$, $\quad (L = \rho l N_A N_B)$.

	E673*	P838	Ratio
l	7.6 cm Be	20 cm LiD	
ρ	1.8 g/cm^3	0.86 g/cm^3 · 0.64(packing fraction)	
N_B	1.2×10^7/min · 60min · 24h · 17 days $\times$ 0.7(ϵ_{beam})	1.17×10^{12}/month $\times$0.8(ϵ_{beam}) · 0.8(ϵ_{exp})	
L	1.7×10^{36} cm^2	5.0×10^{36} cm^2	2.9
$B\sigma$	Common		
$A \cdot \epsilon$	0.03($A_{J/\psi}$) $\times$ 0.8($\epsilon_{J/\psi}$)· 0.16($A_\gamma \cdot \epsilon_\gamma$) $\times$0.6(ϵ_{online}) =2.30×10^{-3} (Trigger eff. is not documented.)	0.43($A_{J/\psi}$)· 0.37(A_γ) $\times$0.88(ϵ_{trig})· 0.5($\epsilon_{J/\psi} \cdot \epsilon_\gamma$) = 0.07	>30
χ_2 yield	11.8 events obtained	$> 11.8 \cdot 2.9 \cdot 30 \simeq 1,030$ events/month	> 87

Scaling the event rate from E673, we expect $\geq$ 1,000 χ_2 events per month for our proposed experiment. Here $A_{J/\psi}$ and A_γ are the acceptances for the J/ψ and γ from the χ_2 decay, and $\epsilon_{J/\psi}$ and ϵ_γ are the respective reconstruction efficiencies.

* Details are from:

P. T. Lukens, Ph.D. Thesis, University of Illinois, 1984, and

T. L. Graff, Ph.D. Thesis, University of Illinois, 1984.

APPENDIX VII

What is Needed from Fermilab for the Next Run

1. Operation of MP beamline for eight months
2. Operation of polarized target and ^{4}He liquifier: same as the 1990 E-704 run
3. PREP items for the additional 1,000 lead glass counters: ADC's, HV supplies
4. Cables for these counters

What is Needed from the Experimenters for the Next run

		Provider
1)	Additional 1,000 lead-glass counters (already in MP9)	Serpukhov
2)	CsI detector and scintillator pad detector	Japanese University groups
3)	Additional proportional chambers	Iowa, Trieste
4)	PPT related: microwave source, holding coil	Argonne Japanese University groups Saclay

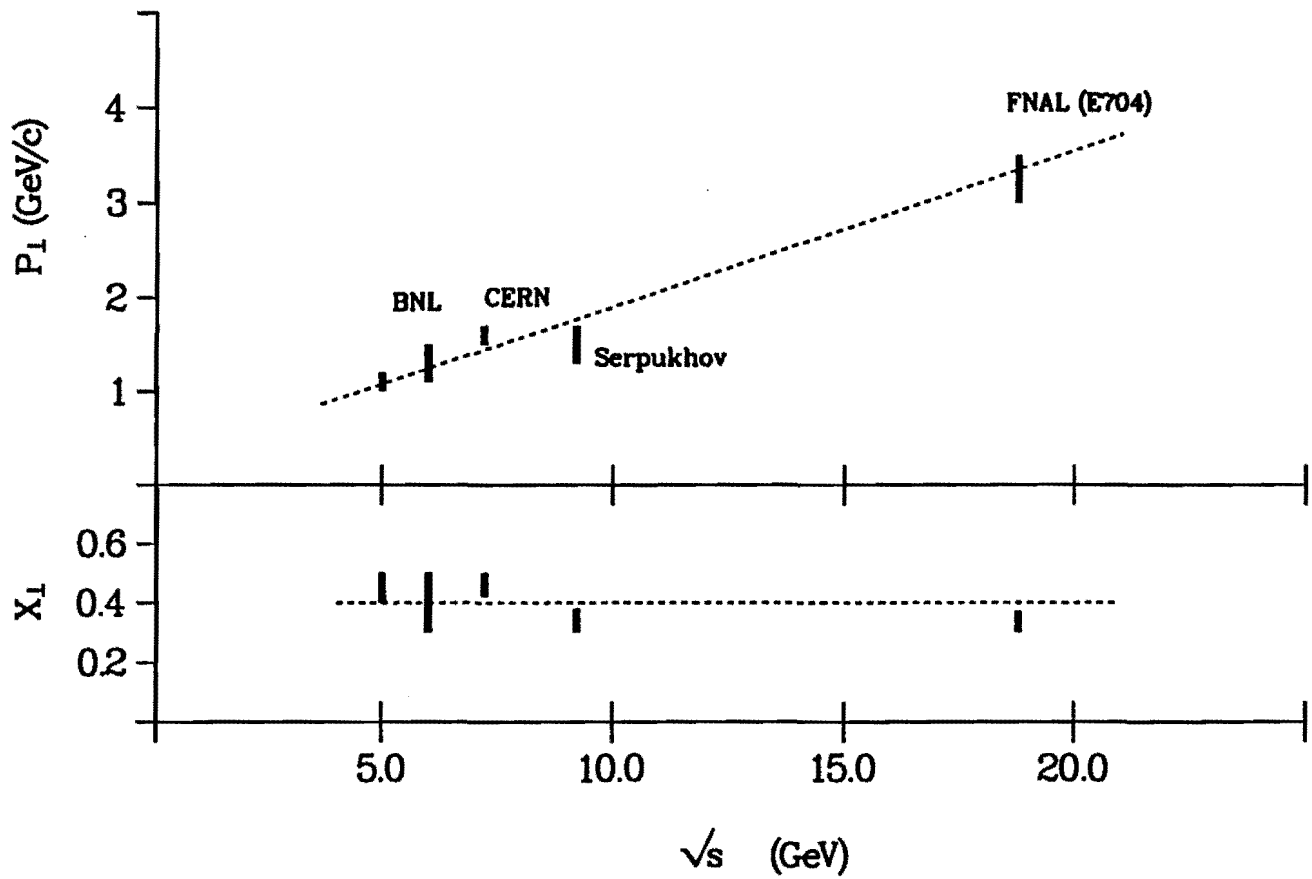

Fig. 1. Demonstration of the x_T scaling in single-spin asymmetry in pion production. Plot of the onset of the rise to large positive values of A_N.

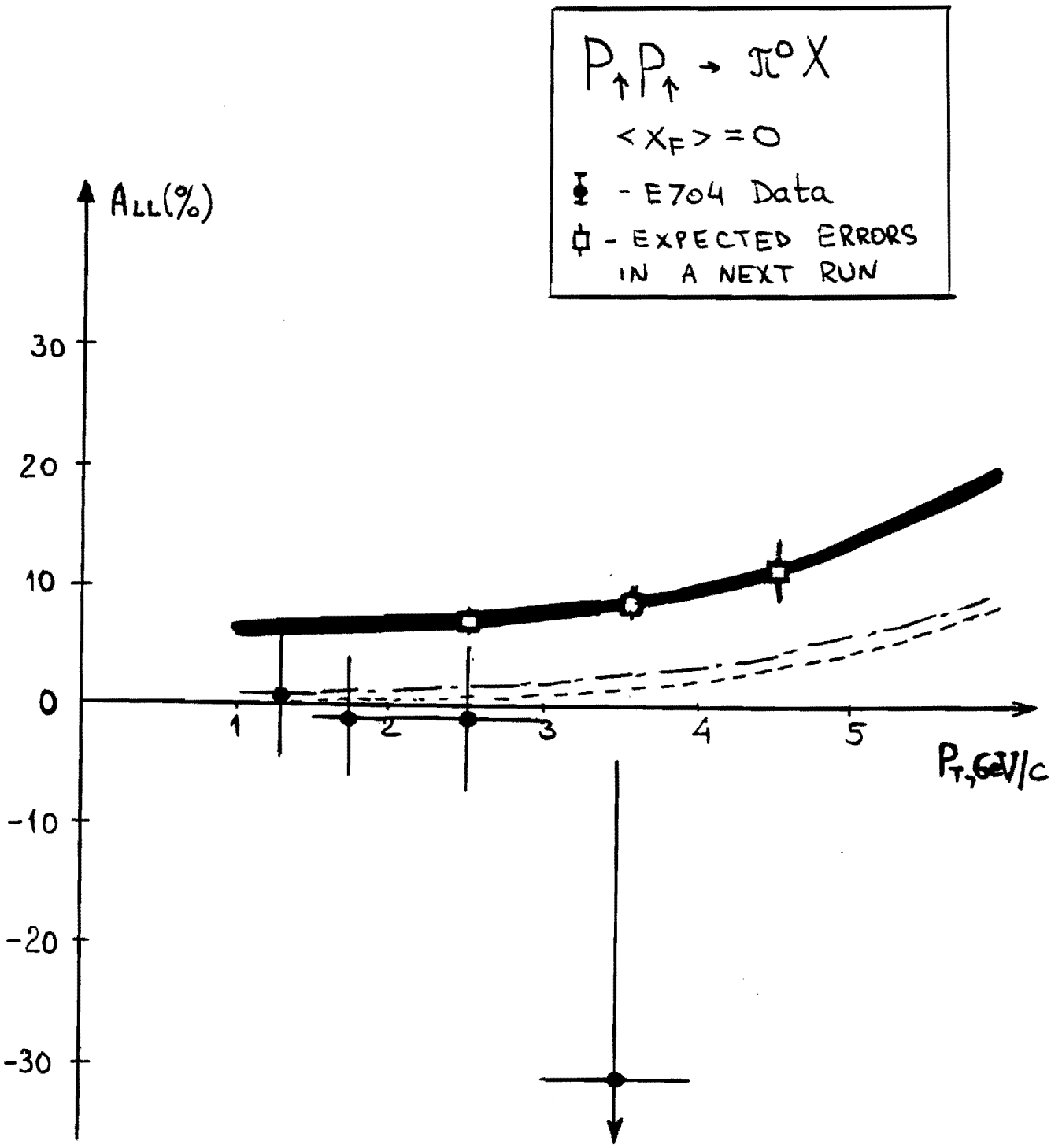

Fig.2. Double-spin Asymmetry, $A_{LL}(p_\uparrow p_\uparrow \to \pi^0 X)$ at 200 GeV.

Curves (from Ref.9):	solid line -	large gluon polarization;
	dot dashed line -	small gluon polarization;
	dashed line -	no gluon polarization.

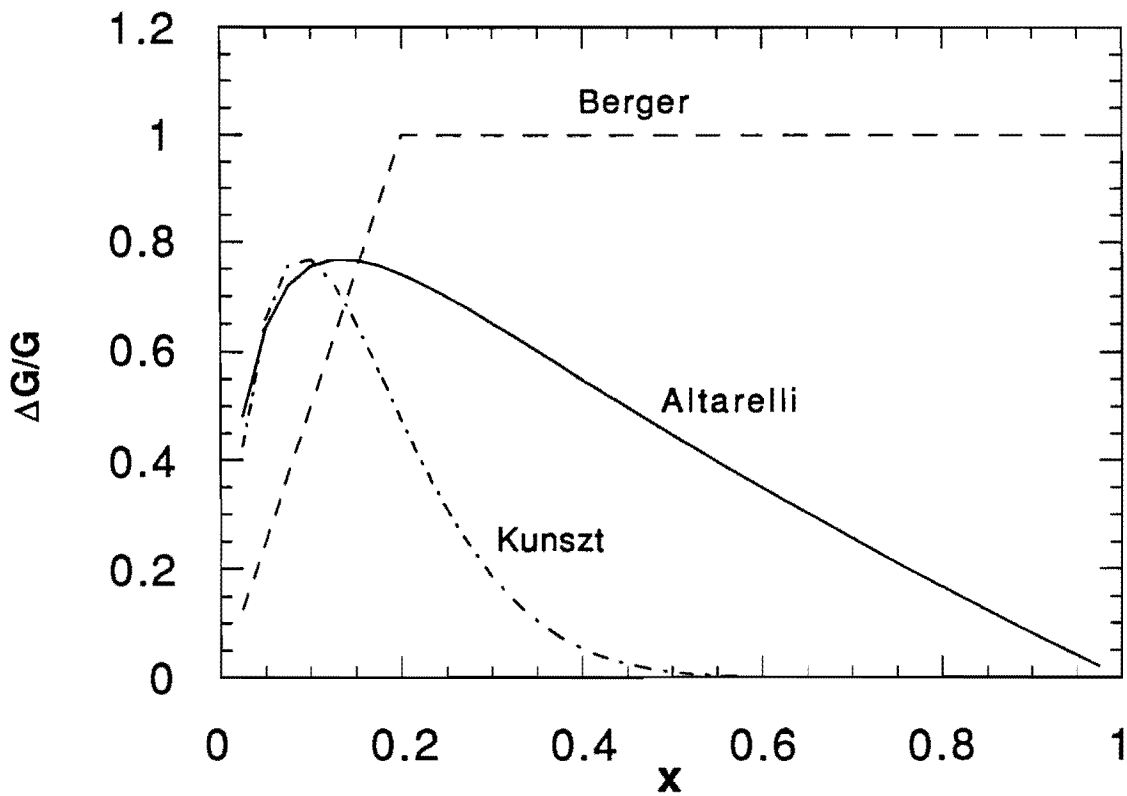

Fig. 3. Assumptions of $\Delta G/G(x)$ (Refs. 12–14).

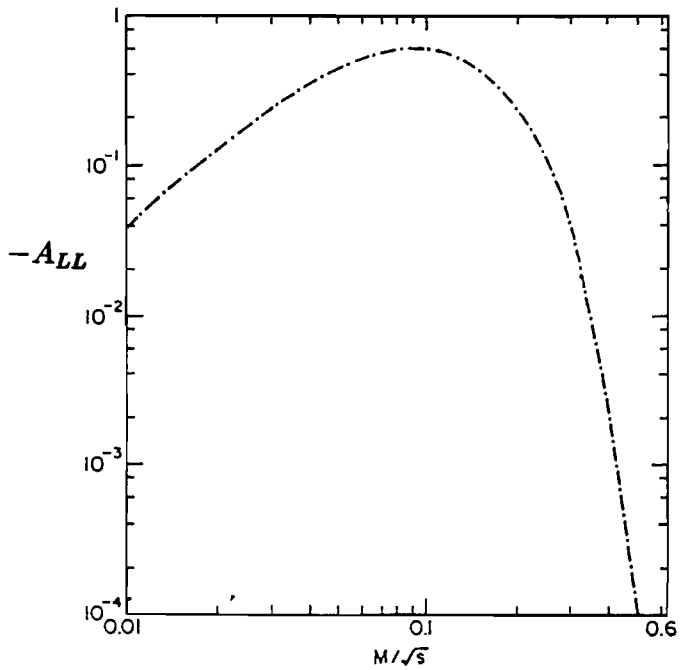

Fig. 4. Prediction of $-A_{LL}$ in χ_2 production[6](see text Section III).

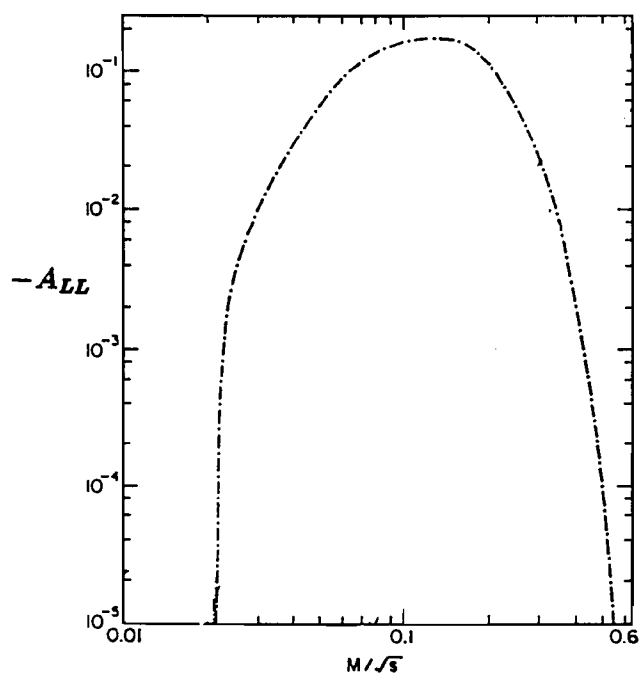

Fig. 5. Prediction of $-A_{LL}$ in J/ψ production[6](see text Section III).

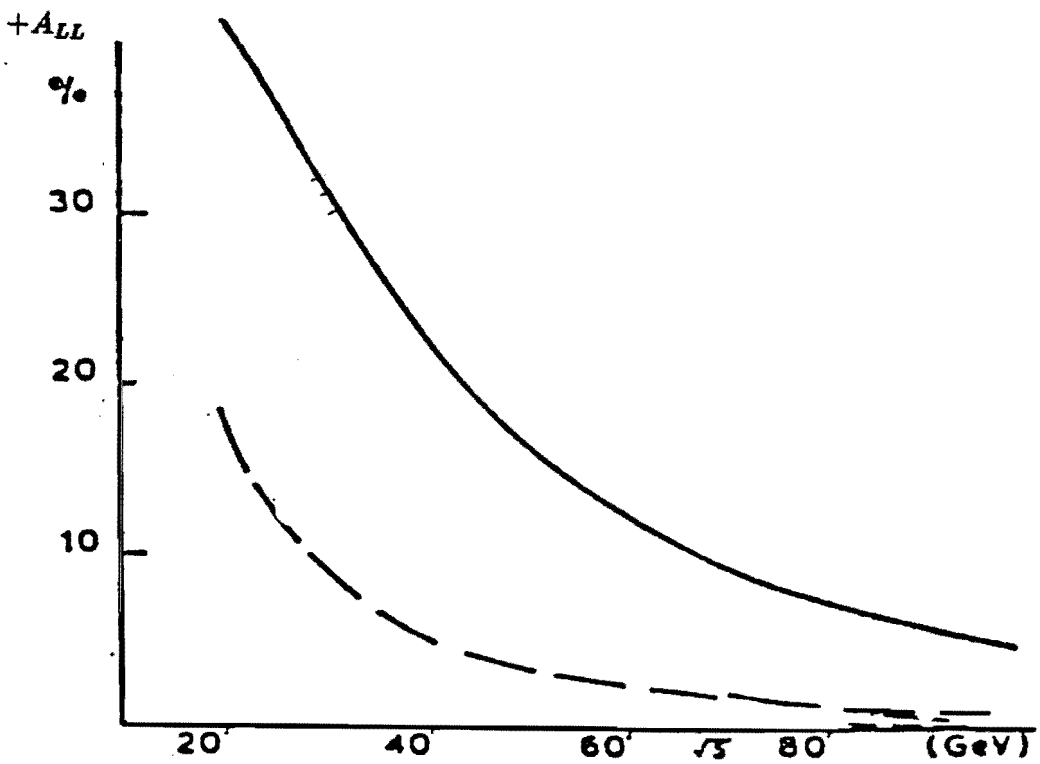

Fig. 6. Prediction of $+A_{LL}$ in charmonium production[11].
Solid line: with large gluon polarization (Ref.12, solution (i)); dashed line: with small gluon polarization + strange quark polarization (Ref.12, solution (ii)).

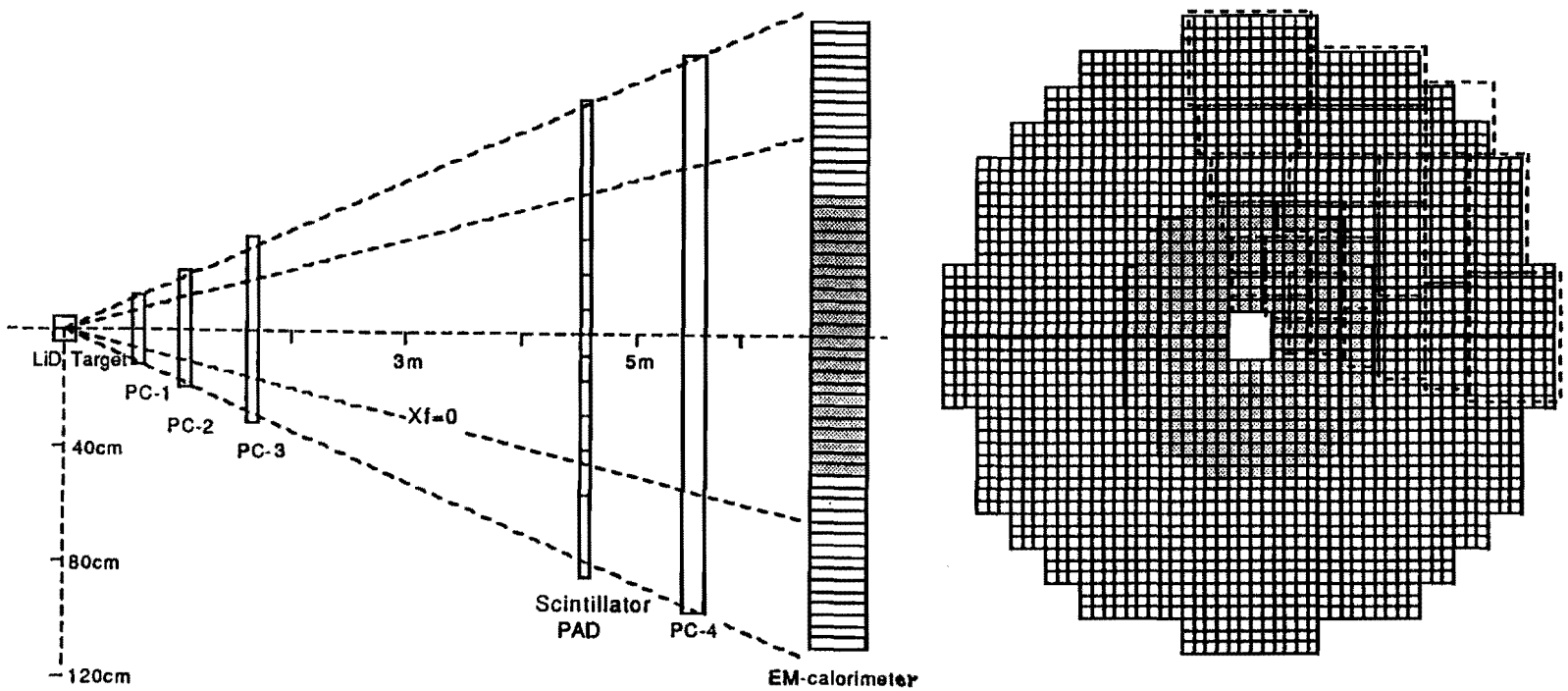

Fig. 7. Schematic view of experimental arrangement; the scintillator pads projected onto the EM calorimeter are shown by dashed lines; CsI blocks are shown in the shaded area.

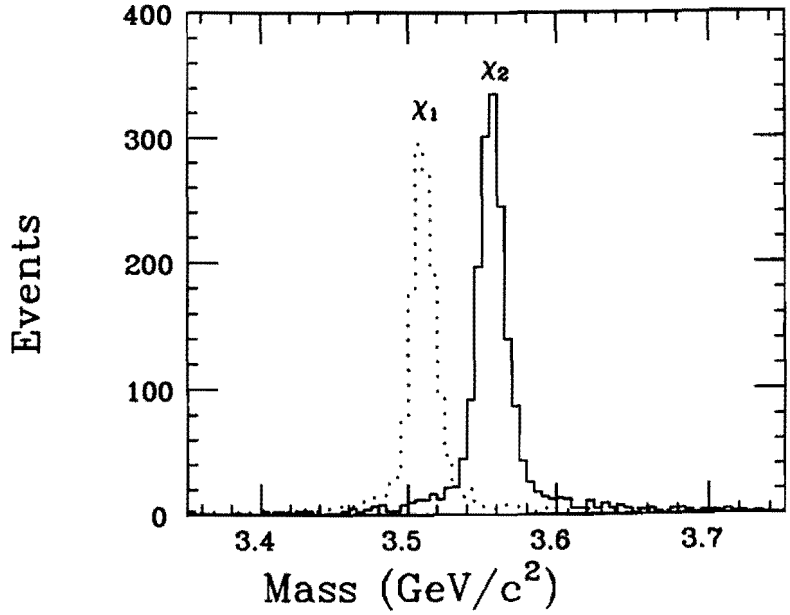

Fig. 8. The χ_1 and χ_2 mass resolution calculated by Monte Carlo methods.

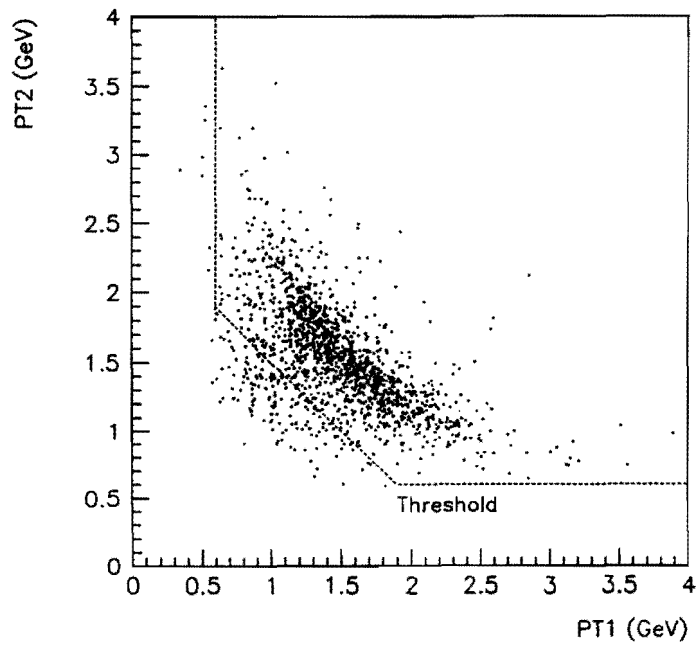

Fig. 9. The p_T correlation between e^+ and e^- from χ_2 decays.

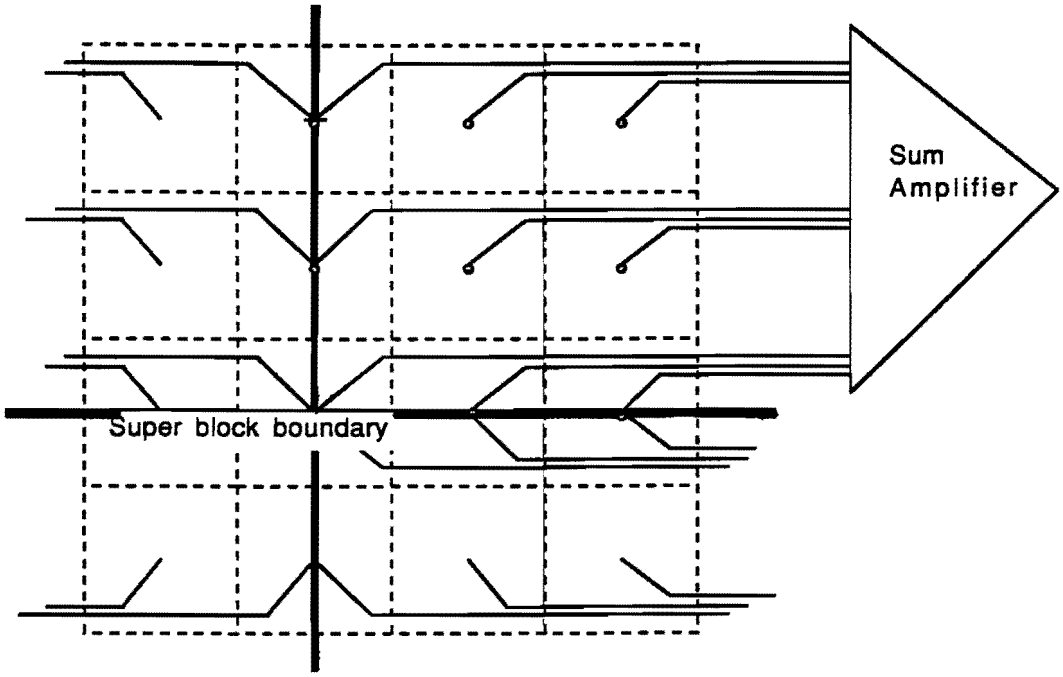

Fig. 10. Schematic view of super-block structure; dashed lines are the calorimeter blocks, and the 2 bold lines are the boundaries of super-blocks.

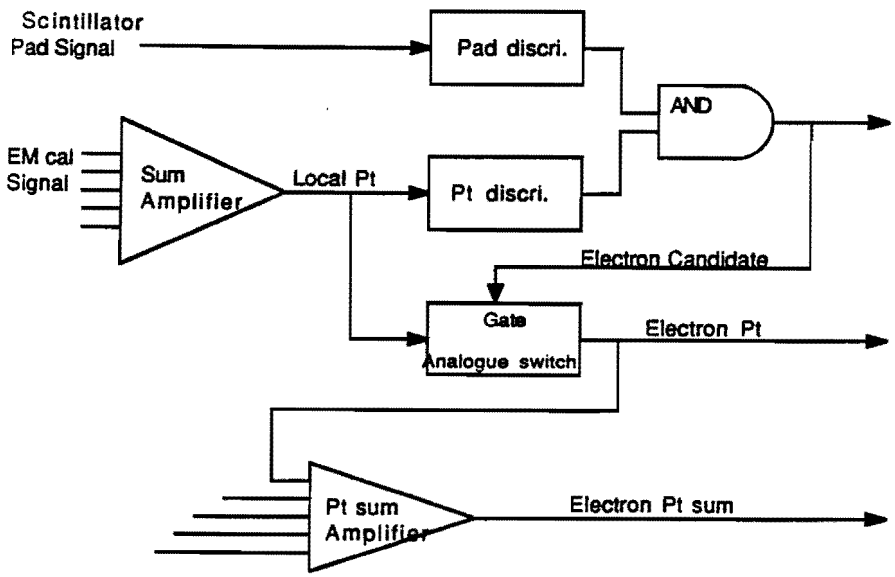

Fig. 11. Logic diagram for J/ψ trigger.

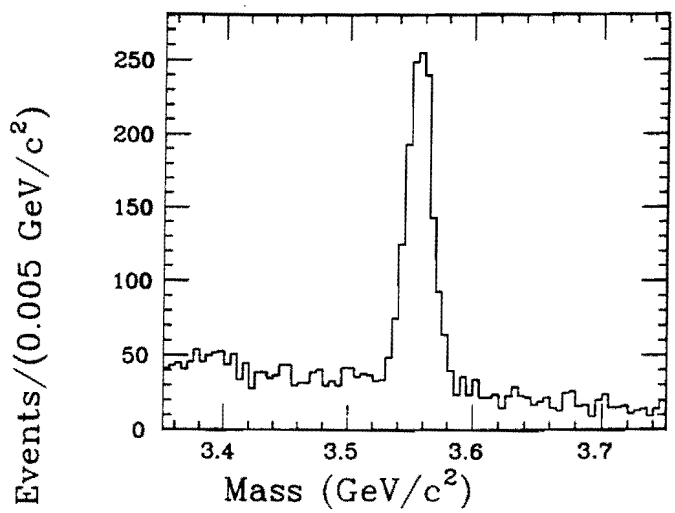

Fig. 12. The $J/\psi + \gamma$ mass spectrum including backgrounds from a Monte Carlo simulation (see text Section VII).

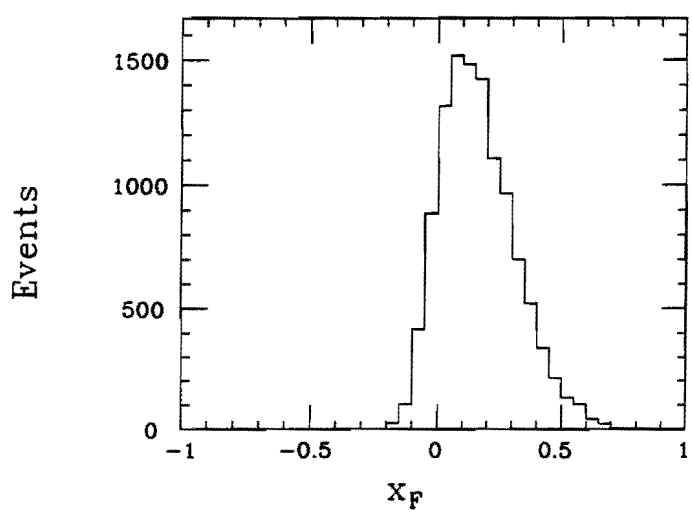

Fig. 13. The x_F distribution of the accepted χ_2 events.

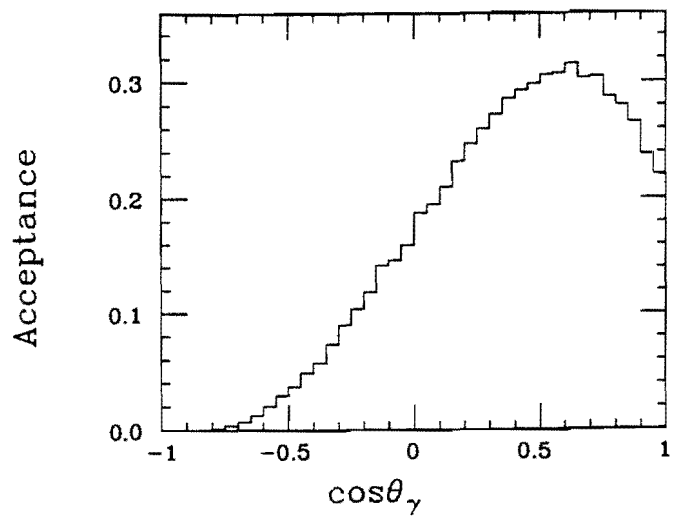

Fig. 14. Angular acceptance of the γ from χ_2 decay.

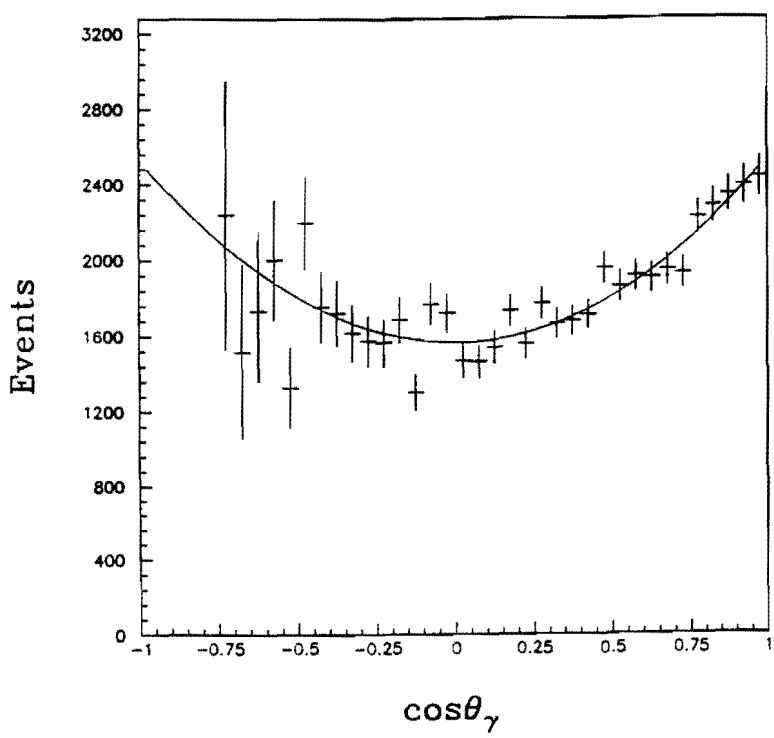

Fig. 15. The $cos\theta_\gamma$ distribution after an acceptance correction. The solid curve is obtained by fitting the distribution with $Eq.(3)$.

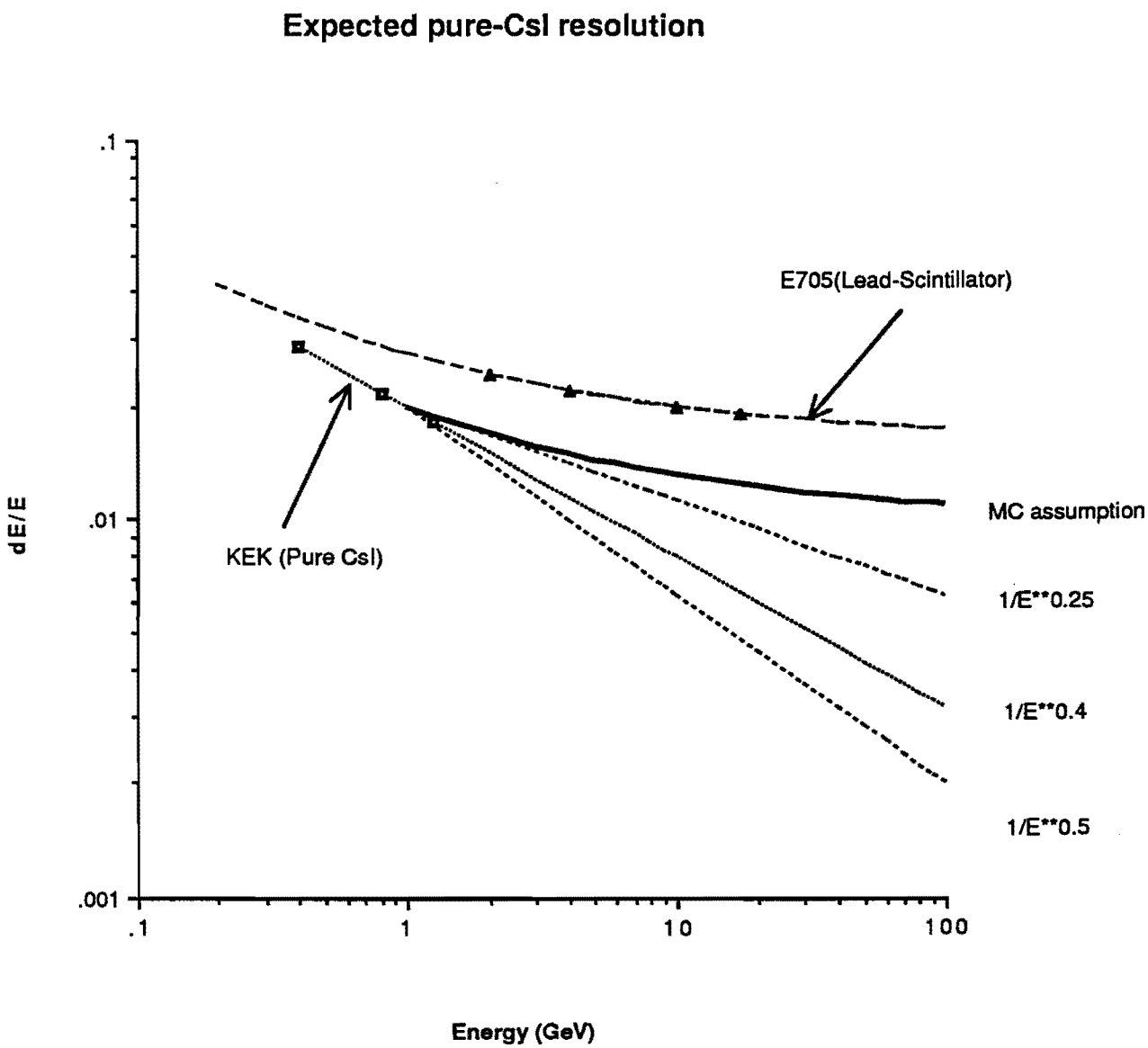

Fig. 16. Expected energy resolution from pure CsI. The solid curve represents our Monte Carlo assumption.